

# Lawrence Berkeley National Laboratory

## Recent Work

### Title

A bonding model for gold(I) carbene complexes.

### Permalink

<https://escholarship.org/uc/item/1gs238n5>

### Journal

Nature Chemistry, 1(6)

### Authors

Benitez, Diego  
Shapiro, Nathan  
Tkatchouk, Ekaterina  
et al.

### Publication Date

2009-09-01

### DOI

10.1038/nchem.331

Peer reviewed



Published in final edited form as:

Nat Chem. 2009 September 1; 1(6): 482–486. doi:10.1038/nchem.331.

## A bonding model for gold(I) carbene complexes

Diego Benitez<sup>1</sup>, Nathan D. Shapiro<sup>2</sup>, Ekaterina Tkatchouk<sup>1</sup>, Yiming Wang<sup>2</sup>, William A. Goddard III<sup>1</sup>, and F. Dean Toste<sup>2,\*</sup>

<sup>1</sup> Materials and Process Simulation Center, California Institute of Technology, Pasadena, California, 91125 USA

<sup>2</sup> Department of Chemistry, University of California, Berkeley, California, 94720 USA

### Abstract

The last decade has witnessed dramatic growth in the number of reactions catalyzed by electrophilic gold complexes. While proposed mechanisms often invoke the intermediacy of gold-stabilized cationic species, the nature of bonding in these intermediates remains unclear. Herein, we propose that the carbon-gold bond in these intermediates is comprised of varying degrees of both  $\sigma$  and  $\pi$ -bonding; however, the overall bond order is generally less than or equal to unity. The bonding in a given gold-stabilized intermediate, and the position of this intermediate on a continuum ranging from gold-stabilized singlet carbene to gold-coordinated carbocation, is dictated by the carbene substituents and the ancillary ligand. Experiments show that the correlation between bonding and reactivity is reflected in the yield of gold-catalyzed cyclopropanation reactions.

---

The unique reactivity of organogold intermediates<sup>1</sup> has recently enabled the development of a wide variety of new carbon-carbon bond forming reactions<sup>2</sup>. Based on the reactivity patterns that have emerged<sup>3</sup>, several mechanistic pathways<sup>4</sup> and bonding models<sup>5</sup> for key intermediates have been proposed, including intermediates ranging from gold carbenes<sup>6</sup> to gold-stabilized carbocations<sup>7</sup>. In the last year, theoretical investigations<sup>8</sup> and experimental observations<sup>9</sup> have further polarized the discussion surrounding the carbenoid or cationic character of organogold species, mostly in support of their carbocationic character<sup>10</sup>. However, gold catalysis has been applied successfully to perform reactions that are traditionally carried out with carbenic systems<sup>11–16</sup>. Given this apparent lack of a consistent and clear understanding of the Au-CR<sub>2</sub><sup>+</sup> bond, we have performed a broad theoretical analysis on key intermediates relevant to gold(I) catalysis. Experimental results in support of our analysis are also presented.

---

Users may view, print, copy, download and text and data- mine the content in such documents, for the purposes of academic research, subject always to the full Conditions of use: [http://www.nature.com/authors/editorial\\_policies/license.html#terms](http://www.nature.com/authors/editorial_policies/license.html#terms)

\*e-mail: [fdtoste@berkeley.edu](mailto:fdtoste@berkeley.edu).

#### Author contributions

DB, NDS and FDT originated the idea and wrote the manuscript; NDS and YW performed the experiments; DB and ET performed the calculations; all authors contributed to discussions and edited the manuscript; DB and NDS contributed equally to this work.

#### Additional information

Supplementary Information accompanies this paper at [www.nature.com/naturechemistry](http://www.nature.com/naturechemistry). Reprints and permission information is available online at <http://npg.nature.com/reprintsandpermissions/>.

The study of carbon–metal multiple bonds has been an area of intense discussion since their conception. For example, after the discovery of rhodium carbenoids, debate ensued as to the nature of the rhodium–carbon bond<sup>17</sup>. While certain calculations and experiments showed that the rhodium–carbon bond order was close to unity, eventually it was accepted, on the basis of reactivity, that a metal–carbon double bond<sup>18</sup> was a more useful and convenient descriptor<sup>19</sup>. A similar discussion has recently emerged concerning the nature of gold–carbon bond. While partially semantic in nature, the correct description is useful for both predicting and explaining reactivity.

## Results and Discussion

### Barrier to bond rotation energy

The magnitude of rotational barriers is a practical way of estimating the strength of  $\pi$ -bonds. Fürstner and co-workers devised a clever experiment to evaluate the carbenic/carbocationic character of (Z)-**AuO**<sup>PPh</sup> and (Z)-**AuOMe**<sup>PMe</sup> by measuring the rotational barrier of bonds adjacent to gold<sup>10</sup>. They concluded that the contribution of the “carbene” resonance was marginal. We used Fürstner’s experiments to validate our theoretical methodology based on the M06 flavor<sup>20</sup> of density functional theory (DFT).

Recently, the M06 flavor of DFT has been shown to accurately describe<sup>21,22</sup> transition metal catalyzed organic transformations. To confirm this, we calculated rotational barriers for (Z)-**AuO**<sup>PPh</sup> and (Z)-**AuOMe**<sup>PMe</sup> (Figure 1) and obtained  $G^\ddagger=10.6$  kcal mol<sup>-1</sup> for (Z)-**AuO**<sup>PPh</sup>, in excellent agreement with experiment ( $G^\ddagger=11.0$ ) and  $G^\ddagger=5.8$  for (Z)-**AuOMe**<sup>PMe</sup>, also consistent with experiment (<7.2 kcal mol<sup>-1</sup>). Previous DFT studies<sup>8</sup> used either B3LYP or BP86 functionals. Although these methods have proven valuable for many organometallic studies, we find that they are insufficient to resolve the issues of interest here. For example, B3LYP predicts rotational barriers of  $G^\ddagger=9.1$  and 7.9 kcal mol<sup>-1</sup>, while BP86 predicts  $G^\ddagger=8.9$  and 7.4 kcal mol<sup>-1</sup> for (Z)-**AuO**<sup>PPh</sup> and (Z)-**AuOMe**<sup>PMe</sup>, respectively. This suggests that both B3LYP and BP86 cannot resolve the effects of the more electron donating **PMe**<sub>3</sub> from the less electron donating **PPh**<sub>3</sub>.

Using our validated computational method, we calculated the barriers to bond rotation for metal-free allyl cations **1**, **2**, and **3**, as well as the gold species (Z)-**AuMe**<sup>PMe</sup>. The results confirm the conclusion of Fürstner and coworkers<sup>10</sup> that the gold-moiety has little effect on the barrier to rotation in (Z)-**AuO**<sup>PPh</sup> ((Z)-**AuO**<sup>PPh</sup> versus **1** ~ 1.4 kcal mol<sup>-1</sup>); however, this conclusion is only valid in the presence of the highly carbocation-stabilizing oxygen atoms. When these heteroatoms are absent, the effect of the gold moiety is quite large ((Z)-**AuMe**<sup>PMe</sup> versus **2** ~ 8.1 kcal mol<sup>-1</sup>). For comparison, the highly stabilizing methoxy group in **3** increases the barrier to rotation by 8.9 kcal mol<sup>-1</sup> versus **2**.

These results suggest that the reactivity of a given gold-stabilized carbene is highly dependent upon the carbene substituents. To gain further insight into the nature of the gold–carbon bond, we examined the structures of these types of intermediates, while varying both carbene and auxiliary ligand substituents.

## Impact of the carbene

As a basis for comparison, we began by calculating the structures and natural atomic charges<sup>23</sup> of metal-free allyl cations **4**, **5**, and **6** (Figure 2a). We also defined parameter  $A$  as the ratio of the bond lengths:  $A \equiv (C^1-C^2)/(C^2-C^3)$ , so that  $A$  indicates roughly whether the partial positive charge on the substrate is more stabilized by its  $C^1$  or  $C^3$  substituents. The low value of  $A$  in **4** (0.926) is indicative of the stabilizing nature of the oxygen lone pairs. The magnitude of  $A$  increases with less-donating  $C^3$ -methyl substituents ( $A = 0.955$ ) and even further for ester-substituted substrate **6** ( $A = 0.983$ ). The corresponding gold-coordinated structures  $\text{Au}_O^{\text{PMe}}$ ,  $\text{Au}_{\text{Me}}^{\text{PMe}}$  and  $\text{Au}_E^{\text{PMe}}$ , all show increased  $A$  values as a result of the ability of the gold moiety to stabilize positive charge at  $C^1$ . In  $\text{Au}_{\text{Me}}^{\text{PMe}}$ ,  $A$  is close to 1 (0.993), suggesting that a secondary gold-stabilized carbocation is as stabilized as a tertiary carbocation. For the diester-substituted allyl carbene  $\text{Au}_E^{\text{PMe}}$ , the  $\pi$  system is now polarized towards the electron deficient  $C^3$  leading to  $A=1.029$ . Importantly, the magnitude of stabilization from the gold-moiety increases with increasing electrophilicity of the allyl-cation. This conclusion can also be reached by considering the natural atomic charge on  $C^3$ . This charge is essentially unaffected in **4** (0.86) versus  $\text{Au}_O^{\text{PMe}}$  (0.83), while it is significantly reduced in **5** (0.43) versus  $\text{Au}_{\text{Me}}^{\text{PMe}}$  (0.34) and **6** (0.21) versus  $\text{Au}_E^{\text{PMe}}$  (0.10).

In order to examine the bonding and reactivity of non-vinyl gold(I) intermediates, we also examined gold alkylidene **7** and compared it to the gold vinyl carbene species (Figure 2b). Our results show that the gold-carbon bond distance (2.057 Å) varies little from the vinyl carbenes. However, in the absence of a delocalized neighboring vinyl group, the Au-C bond possesses a higher  $\pi$ -character, with decreased  $\sigma$ -donation from alkylidene to gold<sup>24</sup>. This demonstrates the ability of the gold moiety to stabilize carbenes of varying electrophilicity by modulating the nature of the gold carbon bond.

A direct consequence of the differences between  $\text{Au}_O^{\text{PMe}}$  and  $\text{Au}_{\text{Me}}^{\text{PMe}}$  is the increased barrier to  $C^2-C^3$  bond rotation in  $\text{Au}_{\text{Me}}^{\text{PMe}}$  (Figure 1). In addition, a difference in reactivity could be expected:  $\text{Au}_O^{\text{PMe}}$  may react as a gold-stabilized carbocation, while  $\text{Au}_{\text{Me}}^{\text{PMe}}$  may react more as a gold-stabilized carbene. We tested and confirmed this hypothesis experimentally. We were unable to observe productive cyclopropanation of intermediates resulting from the gold-catalyzed reaction of cyclopropene **8** (as a precursor to  $\text{Au}_O^{\text{PMe}}$ , Figure 3a). On the other hand, gold-catalyzed reaction of cyclopropene **9** (which should decompose to an intermediate similar to  $\text{Au}_{\text{Me}}^{\text{PMe}}$ ) with *cis*-stilbene provided the product of stereospecific olefin cyclopropanation (Figure 3b). As the yield of this reaction was highly dependent on the auxiliary ligand, we next examined the effect of this ligand on nature of the Au-C1 bond.

## Impact of the ligand<sup>1,25</sup>

The computed structures of  $\text{Au}_{\text{Me}}^{\text{L}}$ , for various ligands (L) are shown in Figure 3c. The L-Au- $C^1$  bonding network can be partitioned into three components (Figure 3d)<sup>26,27</sup>. Since there is only one vacant valence orbital on Au (6s), the Pauli exclusion principle tells us that a 3c/4e  $\sigma$ -hyperbond<sup>28</sup> (where hyperbond refers to bonding beyond the reduced 12e valence space) must be formed for the P-Au-C triad as [P:Au-C $\leftrightarrow$ P-Au:C] (or C-Au-C triad for NHC ligand). As a result, the Au-C1 bond order decreases with increasing trans ligand  $\sigma$ -

donation (trans influence). In the absence of a trans ligand, the gold–carbon bond in  $\text{AuMe}$  is notably shorter (1.985 Å); whereas, in  $\text{AuMe}^{\text{PMe}_3}$ , the electron donating  $\text{PMe}_3$  (strong trans influence) results in a correspondingly long Au–C<sup>1</sup> bond length of 2.053 Å.

In addition, the metal center is able to form two  $\pi$ -bonds by donation from perpendicular filled d-orbitals into empty  $\pi$ -acceptors on the ligand and C<sup>1</sup>. While these two bonds are not mutually exclusive, they compete for electron density from gold. As a result, strongly  $\pi$ -acidic ligands decrease back donation to the substrate, resulting in even longer Au–C<sup>1</sup> bonds (2.057 Å for  $\text{AuMe}^{\text{POMe}}$ ). In contrast, the  $\pi$ -donating chloride ligand in  $\text{AuMe}^{\text{Cl}}$  increases back-donation to C<sup>1</sup> resulting in a very short gold–carbon bond (1.969 Å). In general, the strength of the back-donation to C<sup>1</sup> is dependent on both ligand and, (as demonstrated in the previous section) the electrophilicity of the  $\pi$ -acceptor on C<sup>1</sup>.

The impact of these changes on reactivity is directly apparent in the yield of cyclopropanation product (Figure 3b).  $\pi$ -Acidic ligands are expected to increase carbocation-like reactivity by decreasing gold to C<sup>1</sup>  $\pi$ -donation. Accordingly, we found that strongly  $\pi$ -acidic phosphite ligands provide only traces of the desired product and significant polymerization. Conversely, ligands which increase gold to C<sup>1</sup>  $\pi$ -donation are expected to reduce carbocation-like reactivity, while those ligands that decrease C<sup>1</sup> to gold  $\sigma$ -donation should increase carbene-like reactivity. The N-heterocyclic ligand IPr (1,3-bis(2,6-diisopropylphenyl)imidazol-2-ylidene) should affect both of these changes (it is strongly  $\sigma$ -donating and only weakly  $\pi$ -acidic). Gratifyingly, we found that  $\text{IPrAu}^+$  provides the product of stereospecific cyclopropanation in excellent yield and with high diastereoselectivity (80% yield, 11:1 *cis:trans*). Phosphine ligands fell in between these two extremes. Finally, AuCl was unreactive under these conditions.

### Charge distribution

In order to provide a better and more general view of the bonding in gold vinyl carbene species, we calculated natural charge distributions for the ligand (L), Au, and substrate using NBO analyses. Table 1 shows that the charge is relatively equally distributed between the substrate, gold, and the ligand. Across  $\text{AuMe}^{\text{L}}$  and  $\text{AuO}^{\text{L}}$  series the charge on ligand and Au is well correlated: a change in ligand that results in an increase in ligand charge is correlated with a similar decrease in charge on gold, but these changes have little effect on the charge on the substrate. On the other hand, changing the substrate from  $\text{AuMe}^{\text{L}}$  to  $\text{AuO}^{\text{L}}$  results in an increase in substrate charge. This correlates with a decrease in the charges on both Au and ligand. These results again demonstrate that both the ligand and the substrate play important roles in determining the overall electronic structure.

### Bonding and reactivity

The model in Figure 3d for bonding in gold-stabilized carbenes proposes that these intermediates possess highly electron-deficient  $\alpha$ -carbons that are stabilized, to varying degrees, by back-donation from the metal to the vacant  $p\pi$ -orbital of the singlet carbene. This electronic deficiency reduces donation from the filled  $sp^2$   $\sigma$ -orbital of the carbene to the metal, therefore minimizing gold–carbon  $\sigma$ -bonding. Thus, our model suggests that the conversion of a vinylgold intermediate into a gold-stabilized carbene, which is commonly

proposed in gold-catalyzed reactions<sup>29–34</sup>, occurs with an increase in gold–carbon  $\pi$ -bonding and a decrease in the  $\sigma$ -bonding (Figure 4). The bonding situation in these carbene intermediates has often been depicted by two extreme resonance structures: a carbocation with a gold-carbon single bond or a carbene with a gold-carbon double bond. Much like the double “half-bond” model proposed for rhodium-carbenoid intermediates<sup>35,36</sup>, the depiction of a gold-stabilized carbene with a gold-carbon double bond should not be taken as an indication of a bond order of 2; but rather a means to convey that both  $\sigma$  and  $\pi$  components to the bond are present. To illustrate this, we calculated gold-carbon natural bond orders for **AuO**<sup>PMe</sup> (0.53), **AuMe**<sup>PMe</sup> (0.91), and **7** (1.14). Nucleophilic attack on the now highly electrophilic  $p\pi$ -orbital of the carbon adjacent to gold restores the gold-carbon sigma bond<sup>37–39</sup>. In this scenario, divergence towards carbocation-like or carbene-like reactivity may also be influenced by the potential of the nucleophile to intercept the developing positive charge. Alternatively, gold-stabilized carbene intermediates may react with concerted carbene-like reactivity (i.e. cyclopropanation), especially when the gold is coordinated to electron donating ligands.

## Conclusions

We suggest the reactivity in Au(I)-coordinated carbenes is best accounted for by a continuum ranging from metal stabilized singlet carbene to metal-coordinated carbocation. The position of a given gold species on this continuum is largely determined by the carbene substituents and the ancillary ligand. Consideration of the bonding description described herein provides insight into previously reported gold-catalyzed transformations and a basis for the *ab initio* prediction of reactivity, optimization of ligand effects, and design of new gold-catalyzed reactions.

## Methods

Calculations were performed using density functional theory (DFT) with the M06 functional, as implemented in Jaguar 7.640. All calculations used the Hay and Wadt small core-valence relativistic effective-core-potential<sup>41</sup> (ECP) to describe the 1s-3d core electrons of the gold atom, leaving the outer 16 electrons (4s, 4p, 4d, 5s, *etc.*) to be treated explicitly. The LACVP\*\* basis set was used for all geometry optimizations and LACV3P++\*\* (2f) for energies. LACV3P++\*\* (2f) utilizes the LACV3P++\*\* basis set as implemented in Jaguar plus a double-zeta f-shell with exponents from Martin and Sundermann<sup>42</sup>. All electrons were described for all other atoms using the 6-31G\*\* or 6-311++G\*\* basis sets<sup>43,44</sup>. For each optimized structure, the M06 analytic Hessian was calculated to obtain the vibrational frequencies, which in turn were used to obtain the zero point energies and free energy corrections (without translational or rotational components). Solvent corrections were based on single point self-consistent Poisson-Boltzmann continuum solvation calculations for CH<sub>2</sub>Cl<sub>2</sub> ( $\epsilon = 8.93$  and  $R_0 = 2.33$  Å using the PBF45 module in Jaguar).

## Supplementary Material

Refer to Web version on PubMed Central for supplementary material.

## Acknowledgments

FDT gratefully acknowledges NIHGMS (RO1 GM073932), Bristol-Myers Squibb, and Novartis for funding, and Johnson Matthey for the generous donation of AuCl<sub>3</sub>. The MSC computational facilities were funded by grants from ARO-DURIP and ONR-DURIP. DB and ET thank Dr. Robert “Smith” Nielsen for useful suggestions.

## References

1. Gorin DJ, Sherry BD, Toste FD. Ligand effects in homogeneous Au catalysis. *Chem Rev.* 2008; 108:3351–3378. [PubMed: 18652511]
2. Hashmi ASK. Gold-catalyzed organic reactions. *Chem Rev.* 2007; 107:3180–3211. [PubMed: 17580975]
3. Fürstner A, Davies PW. Catalytic carbophilic activation: catalysis by platinum and gold  $\pi$  acids. *Angew Chem, Int Ed.* 2008; 46:3410–3449.
4. Jiménez-Núñez E, Echavarren AM. Gold-catalyzed cycloisomerizations of enynes: a mechanistic perspective. *Chem Rev.* 2008; 108:3326–3350. [PubMed: 18636778]
5. Gorin DJ, Toste FD. Relativistic effects in homogeneous gold catalysis. *Nature.* 2007; 446:395–403. [PubMed: 17377576]
6. Fedorov A, Moret ME, Chen P. Gas-phase synthesis and reactivity of a gold carbene complex. *J Am Chem Soc.* 2008; 130:8880–8881. [PubMed: 18563897]
7. Hashmi ASK. “High noon” in gold catalysis: Carbene versus carbocation intermediates. *Angew Chem, Int Ed.* 2008; 47:6754–6756.
8. Correa A, Marion N, Fensterbank L, Malacria M, Nolan SP, Cavallo L. Golden carousel in catalysis: the cationic gold/propargylic ester cycle. *Angew Chem, Int Ed.* 2008; 47:718–721.
9. Fürstner A, Morency L. On the nature of the reactive intermediates in gold-catalyzed cycloisomerization reactions. *Angew Chem, Int Ed.* 2008; 47:5030–5033.
10. Seidel G, Mynott R, Fürstner A. Elementary steps of gold catalysis: NMR spectroscopy reveals the highly cationic character of a “gold carbenoid. *Angew Chem, Int Ed.* 2009; 48:2510–2513.
11. Johansson MJ, Gorin DJ, Staben ST, Toste FD. Gold(I)-catalyzed stereoselective olefin cyclopropanation. *J Am Chem Soc.* 2005; 127:18002–18003. [PubMed: 16366541]
12. Horino Y, Yamamoto T, Ueda K, Kuroda S, Toste FD. Au(I)-catalyzed cycloisomerizations terminated by sp<sup>3</sup> C–H bond insertion. *J Am Chem Soc.* 2009; 131:2809–2811. [PubMed: 19206518]
13. Lemière G, et al. Generation and trapping of cyclopentenylidene gold species: four pathways to polycyclic compounds. *J Am Chem Soc.* 2009; 131:2993–3006. [PubMed: 19209868]
14. Fructos MR, Belderrain TR, Frémont P, Scott NM, Nolan SP, Díaz-Requejo MM, Pérez PJ. A gold catalyst for carbene-transfer reactions from ethyl diazoacetate. *Angew Chem, Int Ed.* 2005; 44:5284–5288.
15. López S, Herrero-Gómez E, Pérez-Galán P, Nieto-Oberhuber C, Echavarren AM. Gold(I)-catalyzed intermolecular cyclopropanation of enynes with alkenes: trapping of two different gold carbenes. *Angew Chem, Int Ed.* 2005; 45:6029–6032.
16. Fedorov A, Chen P. Electronic effects in the reactions of olefin-coordinated gold carbene complexes. *Organometallics.* 2009; 28:1278–1281.
17. Sheehan SM, Padwa A, Snyder JP. Dirhodium(II) tetracarboxylate carbenoids as catalytic intermediates. *Tetrahedron Lett.* 1998; 39:949–952.
18. Doyle MP. Electrophilic metal carbenes as reaction intermediates in catalytic reactions. *Acc Chem Res.* 1986; 19:348–356.
19. Nowlan DT, Gregg TM, Davies HML, Singleton DA. Isotope effects and the nature of selectivity in rhodium-catalyzed cyclopropanations. *J Am Chem Soc.* 2004; 125:15902–15911. [PubMed: 14677982]
20. Zhao Y, Truhlar DG. Density functionals with broad applicability in chemistry. *Acc Chem Res.* 2008; 41:157–167. [PubMed: 18186612]



21. Truhlar DG. Molecular modeling of complex chemical systems. *J Am Chem Soc.* 2008; 130:16824–16827. [PubMed: 19072065]
22. Zhao Y, Truhlar DG. Benchmark energetic data in a model system for Grubbs II metathesis catalysis and their use for the development, assessment, and validation of electronic structure methods. *J Chem Theory Comput.* 2009; 5:324–333. [PubMed: 26610108]
23. Reed AE, Curtiss LA, Weinhold F. Intermolecular interactions from a natural bond orbital, donor-acceptor viewpoint. *Chem Re.* 1988; 88:899–926.
24. Irikura KK, Goddard WA III. Energetics of third-row transition metal methyldiene ions  $MCH_2^+$  ( $M = La, Hf, Ta, W, Re, Os, Ir, Pt, Au$ ). *J Am Chem Soc.* 1994; 116:8733–8740.
25. Padwa A, Austin DJ. Ligand effects on the chemoselectivity of transition metal catalyzed reactions of  $\alpha$ -diazo carbonyl compounds. *Angew Chem Int Ed Engl.* 1994; 33:1797–1815.
26. Dewar M. *Bull Soc Chim Fr.* 1951; 18:C71–C77.
27. Chatt J, Duncanson LA. Olefin co-ordination compounds. Part III. Infra-red spectra and structure: attempted preparation of acetylene complexes. *J Chem Soc.* 1953:2939–2947.
28. Landis CR, Weinhold F. Valence and extra-valence orbitals in main group and transition metal bonding. *J Comput Chem.* 2007; 28:198–203. [PubMed: 17063478]
29. Mamane V, Gress T, Krause H, Fürstner A. Platinum- and gold-catalyzed cycloisomerization reactions of hydroxylated enynes. *J Am Chem Soc.* 2004; 126:8654–8655. [PubMed: 15250709]
30. Luzung MR, Markham JP, Toste FD. Catalytic isomerization of 1,5-enynes to bicyclo[3.1.0]hexenes. *J Am Chem Soc.* 2004; 126:10858–10859. [PubMed: 15339167]
31. Gorin DJ, Davis NR, Toste FD. Gold(I)-catalyzed intramolecular acetylenic Schmidt reaction. *J Am Chem Soc.* 2005; 127:1126–1127. [PubMed: 15669852]
32. Nieto-Oberhuber C, Muñoz MP, Buñuel E, Nevado C, Cárdenas DJ, Echavarren AM. Cationic gold(I) complexes: highly alkynophilic catalysts for the exo- and endo-cyclization of enynes. *Angew Chem, Int Ed.* 2004; 43:2402–2406.
33. Shapiro ND, Toste FD. Rearrangement of alkynyl sulfoxides catalyzed by gold(I) complexes. *J Am Chem Soc.* 2007; 129:4160–4161. [PubMed: 17371031]
34. Zhang G, Zhang L. Au-containing all-carbon 1,3-dipoles: generation and [3+2] cycloaddition reactions. *J Am Chem Soc.* 2008; 130:12598–12599. [PubMed: 18754587]
35. Snyder JP, Padwa A, Stengel T, Arduengo AJ III, Jockisch A, Kim H. A stable dirhodium tetracarboxylate carbenoid: crystal structure, bonding analysis, and catalysis. *J Am Chem Soc.* 2001; 123:11318–11319. [PubMed: 11697986]
36. Costantino G, Rovito R, Macchiarulo A, Pellicciari R. Structure of metal-carbenoid intermediates derived from the dirhodium(II)tetracarboxylate mediated decomposition of  $\alpha$ -diazocarbonyl compounds: a DFT study. *J Mol Struct Theochem.* 2002; 581:111.
37. Amijs CHM, López-Carrillo V, Echavarren AM. Gold-catalyzed addition of carbon nucleophiles to propargyl carboxylates. *Org Lett.* 2007; 9:4021–4024. [PubMed: 17764193]
38. Davies PW, Albrecht SJ-C. Alkynes as masked ylides: gold-catalysed intermolecular reactions of propargylic carboxylates with sulfides. *Chem Commun.* 2008:238–240.
39. Nieto-Oberhuber C, Muñoz MP, López S, Jiménez-Núñez E, Nevado C, Herrero-Gómez E, Raducan M, Echavarren AM. Gold(I)-catalyzed cyclizations of 1,6-enynes: alkoxy cyclizations and exo/endo skeletal rearrangements. *Chem Eur J.* 2006; 12:1677–1693. [PubMed: 16358351]
40. Jaguar 7.6. Schrodinger, LLC; New York, NY: 2006.
41. Hay PJ, Wadt WR. Ab initio effective core potentials for molecular calculations - potentials for K to Au including the outermost core orbitals. *J Chem Phys.* 1985; 82:299–310.
42. Martin JML, Sundermann A. Correlation consistent valence basis sets for use with the Stuttgart-Dresden-Bonn relativistic effective core potentials: The atoms Ga-Kr and In-Xe. *J Chem Phys.* 2001; 114:3408–3420.
43. Krishnan R, Binkley JS, Seeger R, Pople JA. Self-consistent molecular-orbital methods. XX A basis set for correlated wave-functions. *J Chem Phys.* 1980; 72:650–654.
44. Frisch MJ, Pople JA, Binkley JS. Self-consistent molecular-orbital methods 25. Supplementary functions for Gaussian-basis sets. *J Chem Phys.* 1984; 80:3265–3269.



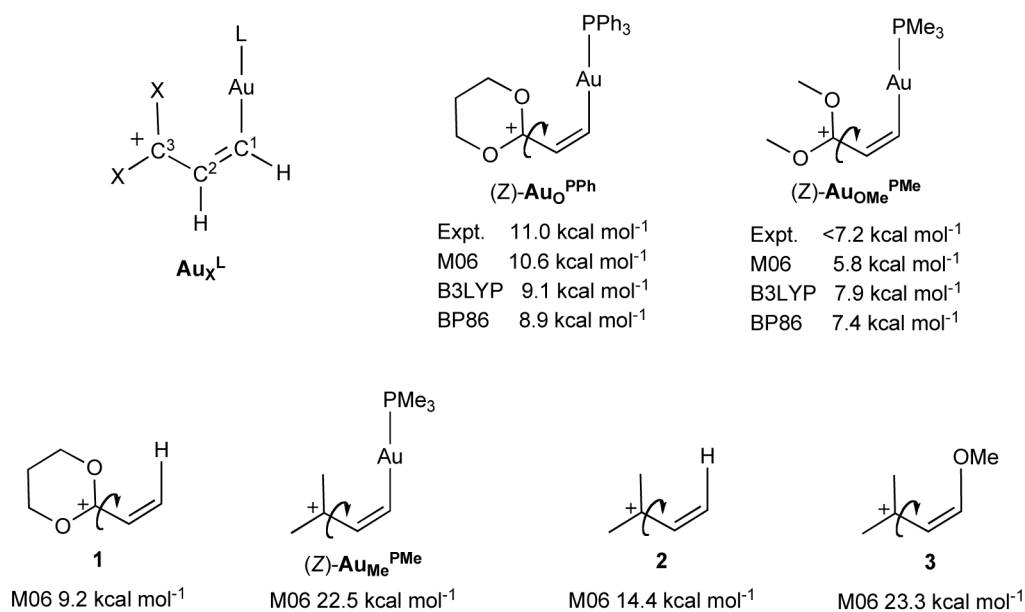
45. Tannor DJ, et al. Accurate first principles calculation of molecular charge-distributions and solvation energies from ab-initio quantum-mechanics and continuum dielectric theory. *J Am Chem Soc.* 1994; 116:11875–11882.

Author Manuscript

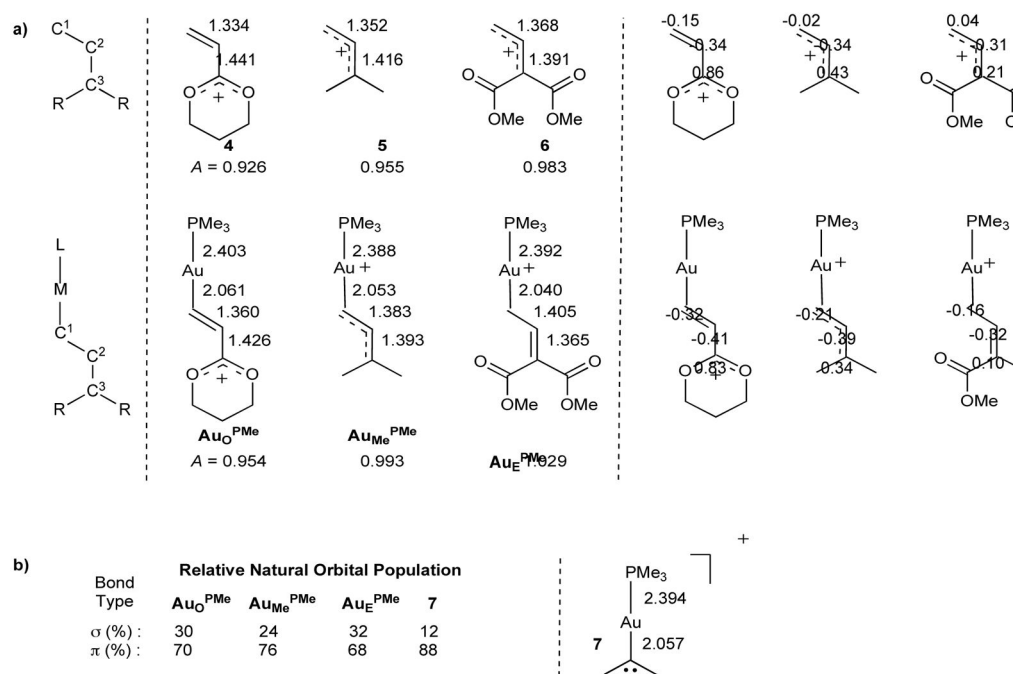
Author Manuscript

Author Manuscript

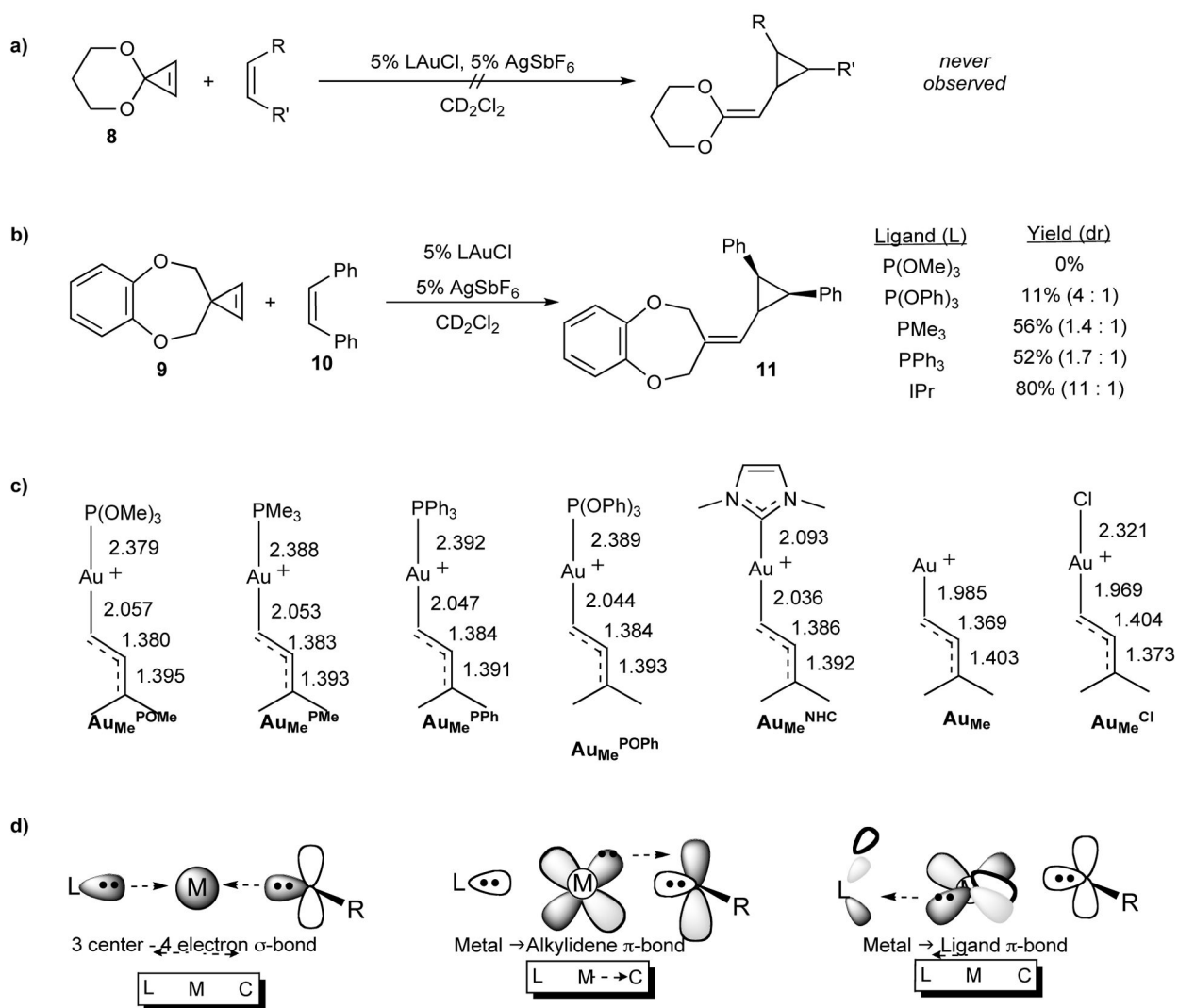
Author Manuscript

**Figure 1.**

Calculated and experimental activation energies to bond rotation (indicated with arrows). C<sup>3</sup>-C<sup>2</sup> bond rotation barriers are decreased when C<sup>3</sup> is substituted with carbocation-stabilizing oxygen atoms. Throughout the text gold complexes will be referred to according to the **Au<sub>X</sub><sup>L</sup>** notation, where L indicates the auxiliary ligand on gold and X indicates the C<sup>3</sup> substituents (Me = methyl, O = 1,3-dioxanyl, OMe = methoxy, E = methyl ester).

**Figure 2.**

Structural and electronic comparison of cationic metal-free and  $[AuPMe_3]^+$  substituted substrates. (a) On the left, calculated bond distances ( $\text{\AA}$ ), and on the right, natural charges for  $C^1$ ,  $C^2$ , and  $C^3$ . Parameter  $A$  is defined as the ratio of bond distances  $(C^1-C^2)/(C^2-C^3)$  and correlates to the polarization of the  $\pi$ -electrons along the delocalized  $C^1-C^2-C^3$  system. (b) A comparison of with Au-alkylidene **7** showing the relative natural orbital populations of  $\sigma$  and  $\pi$  contributions to the Au-C bond. On the right calculated bond distances ( $\text{\AA}$ ) for **7**.

**Figure 3.**

Experimental and theoretical comparison for the carbene reactivity of the substrate with different ancillary ligands. (a) Attempted and (b) observed carbene-like reactivity, demonstrating the impact of the auxiliary ligand on the yield of cyclopropanation product. (c) Bond distances in Au<sub>Me</sub><sup>L</sup> complexes. (d) A stylized depiction of the most important bonding interactions in L-Au(I)-CR<sub>2</sub><sup>+</sup> species.

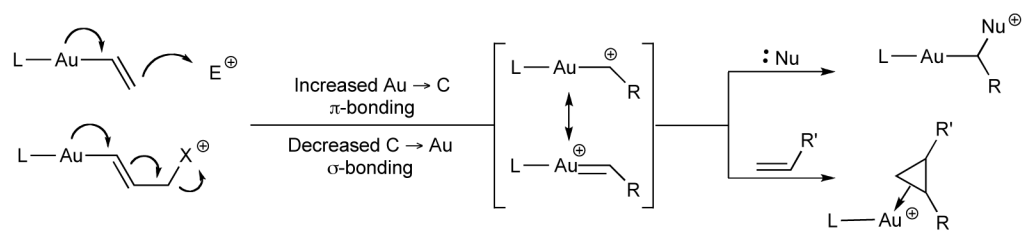


**Figure 4.**

Arrow pushing in the formation of gold-stabilized carbenes is a useful mnemonic for keeping track of electrons, but it can lead to misconceptions about bonding. While the Au-C bond in the intermediate carbene has both  $\sigma$  and  $\pi$  components, the overall bond order is generally less than or equal to unity.

**Table 1**

Calculated natural populations (charge) for the ancillary ligand, gold atom, and substrate.

	$\text{Au}_{\text{NHC}}^{\text{NHC}}$	$\text{Au}_{\text{NHC}}^{\text{PMe}}$	$\text{Au}_{\text{NHC}}^{\text{POMe}}$	$\text{Au}_{\text{O}}^{\text{NHC}}$	$\text{Au}_{\text{O}}^{\text{PMe}}$	$\text{Au}_{\text{O}}^{\text{POMe}}$
Ligand	0.32	0.40	0.45	0.31	0.37	0.42
Metal	0.39	0.30	0.25	0.36	0.27	0.23
Substrate	0.29	0.31	0.31	0.33	0.36	0.35